THE ASTRONOMICAL JOURNAL, 125:3302–3310, 2003 June

HUBBLE SPACE TELESCOPE OBSERVATIONS OF BINARY VERY LOW MASS STARS AND BROWN DWARFS

JOHN E. GIZIS[1]
Department of Physics and Astronomy, University of Delaware, Newark, DE 19716; gizis@udel.edu

I. NEILL REID
Space Telescope Science Institute, 3700 San Martin Drive, Baltimore, MD 21218

GILLIAN R. KNAPP
Department of Astrophysical Sciences, Princeton University, Princeton, NJ 08544-1001

JAMES LIEBERT
Steward Observatory, University of Arizona, 933 North Cherry Avenue, Tucson, AZ 85721

J. DAVY KIRKPATRICK
Infrared Processing and Analysis Center, 100-22, California Institute of Technology, Pasadena, CA 91125

DAVID W. KOERNER
Department of Physics and Astronomy, Northern Arizona University, Box 6010, Flagstaff, AZ 86011-6010

AND

ADAM J. BURGASSER[2]
Division of Astronomy and Astrophysics, 8965 Math Science Building, UCLA, Los Angeles, CA 90095-1562
Received 2002 October 25; accepted 2003 February 21

ABSTRACT

We present analysis of *Hubble Space Telescope* (*HST*) images of 82 nearby field late M and L dwarfs. We resolve 13 of these systems into double M/L dwarf systems and identify an additional possible binary. Combined with previous observations of 20 L dwarfs, we derive an observed binary fraction for ultracool dwarfs of $17^{+4}_{-3}\%$, where the statistics included systems with separations in the range 1.6–16 AU. We argue that accounting for biases and incompleteness leads to an estimated binary fraction $15\% \pm 5\%$ in the range 1.6–16 AU. No systems wider than 16 AU are seen, implying that the wide companion frequency is less than 1.7%; the distribution of orbital separation is peaked at ~2–4 AU and differs greatly from the G dwarf binary distribution. Indirect evidence suggests that the binary fraction is $\sim 5\% \pm 3\%$ for separations less than 1.6 AU. We find no evidence for differences in the binary fraction between stellar late M and L dwarfs and substellar L dwarfs. We note, however, that the widest (greater than 10 AU) systems in our sample are all of earlier (M8–L0) spectral type; a larger sample is needed to determine if this is a real effect. One system with a spectral type of L7 has a secondary that is fainter in the *HST* F814W filter but brighter in F1042M; we argue that this secondary is an early T dwarf.

Key words: binaries: general — stars: low-mass, brown dwarfs

1. INTRODUCTION

The Deep Near-Infrared Survey (DENIS; Epchtein 1997; Delfosse et al. 1997), Two Micron All-Sky Survey (2MASS; Skrutskie et al. 1997; Cutri et al. 2000),[3] and Sloan Digital Sky Survey (SDSS; York et al. 2000) have enabled the discovery of numerous cool dwarfs and led to the definition of new spectral types L (Kirkpatrick et al. 1999; Martín et al. 1999b) and T (Burgasser et al. 2002a; Geballe et al. 2002). With effective temperatures lower than ~2000 and ~1300 K, respectively, these objects span the range between the lowest mass stars and substellar mass brown dwarfs. The latest M dwarfs (M8/M9) and the earlier type L dwarfs represent a mix of brown dwarfs, which are still cooling, and long-lived hydrogen-burning stars, which have reached a stable state (Reid et al. 1999). Theoretical models indicate that the overwhelming majority of L dwarfs with temperature below ~1750 K (spectral types ≈L5 and later; Kirkpatrick et al. 1999; Gizis et al. 2000), and all T dwarfs, are expected to be brown dwarfs.

The large samples now available of these objects allow investigation of their statistical characteristics. One goal of such studies is the establishment of empirical constraints on the formation mechanism(s) of low-mass dwarfs, particularly searching for potential differences in the properties of the lowest mass stars and brown dwarfs. It is clear that the properties of binary brown dwarfs are important in this context. A comprehensive theory of star formation must account not only for the stellar/substellar initial mass function (IMF), but also the frequency and orbital distributions of binary systems. Although brown dwarfs are extremely rare as close companions to GFK stars (Halbwachs et al. 2000; Marcy & Butler 2000), a number of studies have detected double brown dwarf systems (Martín, Brandner, &

[1] Visiting Astronomer, Kitt Peak National Observatory, National Optical Astronomy Observatory, which is operated by the Association of Universities for Research in Astronomy (AURA), Inc., under cooperative agreement with the National Science Foundation (NSF).
[2] Hubble Fellow.
[3] See http://www.ipac.caltech.edu/2mass/releases/second/doc/explsup.html.

Basri 1999a; Koerner et al. 1999; Reid et al. 2001; Close et al. 2002a; Burgasser et al. 2003), and even doubles that orbit more massive stars (Martín et al. 2000b; Potter et al. 2002).[4]

The current paper presents analysis of the largest sample of high-resolution images of low-mass dwarfs assembled so far. We have used the Planetary Camera of the Wide Field Planetary Camera 2 (WFPC2) on the *Hubble Space Telescope* (*HST*) to image a sample of 82 late-type M and L dwarfs. Details of those observations are presented in § 2. Comments on individual systems are given in § 3. We have combined our current observations with data for 20 L dwarfs analyzed by Reid et al. (2001), and we use those data to set constraints on the binary fraction in low-mass dwarfs. That analysis is presented in § 4, and our conclusions summarized in the final section.

2. DATA

Targets for snapshot WFPC2 imaging with *HST* were chosen from the list of 2MASS-selected late M dwarfs (Gizis et al. 2000) and L dwarfs (Kirkpatrick et al. 1999, 2000) and from late M and L dwarfs identified from the initial regions covered by SDSS (Fan et al. 2000; Schneider et al. 2002; Hawley et al. 2002). A few 2MASS and SDSS objects included have not yet been described in publications. Near-infrared discovery spectra for 2M0033−1521, 2M0326−2102, and 2M2242+2542 are shown in Figure 1. These data were obtained using the infrared Cryogenic Spectrometer (CRSP) on the Kitt Peak 4 m telescope during observing runs in 1999 February and November. The February data were obtained using grating 2. The setup provided *L*-band spectra from *K*-band spectra from 1.85 to 2.55 μm. In November, we switched to the slightly higher resolution grating 4, which yielded spectra over the range 1.90–2.55 μm at *K* band or 1.05–3.75 μm at *J* band. The resolution, as measured by the FWHM of arc lines, was 55 and 110 Å at *J* and *K*, respectively, for grating 4. Data from this run are discussed in Schweitzer et al. (2002). Observations were obtained in the standard way described in the CRSP User's Manual (Joyce 1999).[5] Each object was stepped along the slit to obtain observations at five positions. When necessary, this cycle was repeated to obtain a higher signal-to-noise ratio. Typical individual exposures were 20 s at *K* band. Spectra were extracted using IRAF. Both the *HST* photometry described below and comparison of these near-IR spectra to 25 optically classified L dwarfs observed with the same setup indicates that they are L dwarfs; however, optical spectra are needed to obtain accurate spectral types.

Each object on the *HST* program was observed at least once using the F814W and F1042M filters. For the brighter targets, a second F814W observation was possible in the time frame allowed by the Snapshot visit. Exposure times in F814W ranged from 40 to 400 s, while exposure times in F1042M were always 500 s. A total of 82 dwarfs were observed (Table 1). In general, Gizis & Reid (1995) found that we are able to resolve systems with magnitude differences of 0, 1, 3, and 5 at separations of 0″.09, 0″.14, 0″.23, and 0″.31, respectively, using WFPC2. It should be noted, however, that in the case of the fainter L dwarfs, necessarily observed with lower signal-to-noise ratio, only companions within 3 mag of the primary are detectable. We searched only the PC chip for companions. Coverage for wider companions is provided by the 2MASS data, which would have detected any companions with $K_s < 14.5$ and wider than a few arcseconds.

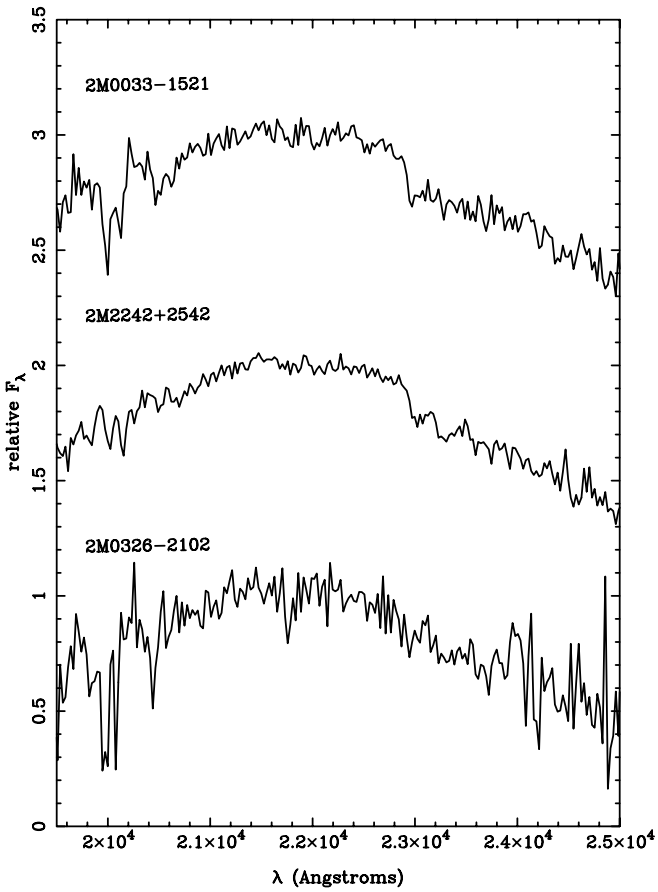

FIG. 1.—KPNO 4 m CRSP spectra of three new L dwarfs. The observations are described in Schweitzer et al. (2002).

Aperture photometry was measured and zero-pointed for each target according to the precepts of Holtzman et al. (1995). However, since we usually have only single frames in each filter, we found that the large aperture magnitudes were often contaminated by cosmic rays. Furthermore, the aperture magnitudes cannot be used for close doubles. DAOPHOT/IRAF was therefore used to measure magnitudes by fitting a point-source function (PSF) model, which was built using images of bright, single stars from this program. The PSF-subtracted images were an effective way of verifying that no secondaries were missed in the apparently single stars. The normalization between the DAOPHOT magnitudes and the aperture magnitudes was determined by taking the median value for high signal-to-noise ratio, isolated stars. Finally, we corrected for charge transfer efficiency (CTE) losses using Dolphin's (2000) *Y*-CTE corrections and *X*-CTE corrections. The resulting magnitudes for each system are given in Table 1. This table includes 2MASS Version 2 Working Database (corresponding to the Second Incremental Data Release system) JHK_s magnitudes for all systems. None of the binaries were resolved by 2MASS, so the magnitudes listed reflect the combined photometry.

[4] After the initial submission of this paper, Close et al. (2003) reported the independent discovery that 2M1127+74AB and 2M1311+80AB are doubles.

[5] See http://www.noao.edu/kpno/manuals/crsp/.

TABLE 1
TARGET SYSTEMS

Name	I	Z	J	H	K_s	σ_I	σ_Z	σ_J	σ_H	σ_K	d (pc)	No.	Ref.
2MASS J03264225−2102057	19.977	17.422	16.111	14.774	13.885	0.027	0.091	0.100	0.075	0.062	14	1	1
2MASS J08564793+2235182	19.096	16.888	15.647	14.579	13.924	0.041	0.039	0.061	0.055	0.050	35	1	2
2MASS J00100368+3436099	18.231	16.332	15.642	15.080	14.391	0.026	0.059	0.066	0.089	0.073	97	1	3
2MASS J00283943+1501418	20.439	17.970	16.477	15.226	14.539	0.042	0.127	0.109	0.086	0.071	12	1	4
2MASS J00303013−1450333	20.286	17.752	16.325	15.283	14.492	0.029	0.101	0.115	0.102	0.097	11	1	4
2MASS J00332386−1521309	18.718	16.612	15.294	14.225	13.397	0.020	0.058	0.055	0.043	0.040	31	1	1
2MASS J02085499+2500488	17.196	15.083	14.015	13.110	12.579	0.017	0.031	0.032	0.035	0.037	27	1	4
2MASS J02243670+2537042	19.760	17.722	16.550	15.419	14.670	0.034	0.086	0.107	0.083	0.085	83	1	4
2MASS J03284265+2302051	20.434	17.493	16.556	15.547	14.833	0.031	0.111	0.155	0.132	0.105	17	1	4
2MASS J03350208+2342356	14.687	...	12.259	11.654	11.261	0.021	...	0.028	0.033	0.025	21	1	5
2MASS J03370359−1758079	19.405	17.019	15.594	14.412	13.588	0.021	0.058	0.065	0.051	0.047	13	1	4
2MASS J03454316+2540233	17.244	14.996	13.992	13.170	12.665	0.034	0.020	0.028	0.034	0.029	27.0	1	3
2MASS J03505737+1818069	15.603	13.733	12.951	12.222	11.763	0.017	0.022	0.031	0.034	0.032	28	1	5
2MASS J03554191+2257016	19.545	17.318	16.099	15.023	14.247	0.024	0.064	0.087	0.075	0.066	43	1	3
2MASS J07533217+2917119	18.802	16.595	15.485	14.489	13.849	0.022	0.046	0.049	0.047	0.055	42	1	4
2MASS J08014056+4628498	19.757	17.356	16.287	15.439	14.540	0.029	0.069	0.140	0.146	0.112	45	1	4
2MASS J08295707+2655099	20.774	18.238	17.109	15.723	14.685	0.028	0.113	0.201	0.140	0.081	40	1	4
2MASS J08320451−0128360	17.388	15.283	14.127	13.309	12.687	0.023	0.026	0.028	0.027	0.031	25	1	4
2MASS J09141884+2238134	18.391	16.280	15.304	14.396	13.898	0.021	0.036	0.047	0.045	0.041	56	1	3
2MASS J09510549+3558021	20.971	18.177	17.358	15.894	14.966	0.026	0.143	0.256	0.155	0.101	52	1	4
2MASS J10170754+1308398	17.414	15.275	14.126	13.194	12.683	0.040	0.047	0.033	0.034	0.032	30	2	6
2MASS J11023375−2359464	20.812	18.398	17.040	15.614	14.794	0.025	0.114	0.193	0.125	0.112	29	1	4
2MASS J11040127+1959217	17.981	15.751	14.369	13.492	12.974	0.019	0.028	0.031	0.038	0.038	13	1	2
2MASS J11083081+6830169	16.554	...	13.139	12.227	11.600	0.027	...	0.027	0.024	0.031	12	1	5
2MASS J11122567+3548131	18.144	15.990	14.573	13.473	12.694	0.064	0.075	0.043	0.041	0.046	16	1	4
2MASS J11275346+7411076	15.812	13.871	13.059	12.367	11.971	0.041	0.032	0.031	0.028	0.029	36	2	5
2MASS J12391934+2029519	17.326	15.225	14.465	13.611	13.116	0.018	0.035	0.034	0.038	0.036	49	1	3
2MASS J12392727+5515371	18.338	16.009	14.670	13.539	12.743	0.032	0.060	0.033	0.036	0.031	19	2	4
2MASS J13113921+8032219	15.458	13.552	12.784	12.116	11.721	0.039	0.037	0.022	0.025	0.024	33	2	5
2MASS J14032232+3007547	15.415	13.482	12.691	12.008	11.626	0.024	0.027	0.026	0.028	0.026	24	1	5
2MASS J14111735+3936363	17.871	15.691	14.641	13.757	13.244	0.049	0.037	0.039	0.041	0.035	33	1	4
2MASS J14263161+1557012	15.823	13.774	12.868	12.182	11.709	0.039	0.040	0.031	0.036	0.033	26	2	5
2MASS J14304358+2915405	17.583	15.406	14.279	13.420	12.746	0.041	0.041	0.029	0.033	0.030	36	2	2
2MASS J14342644+1940499	18.206	16.249	15.561	14.810	14.389	0.017	0.037	0.063	0.081	0.074	92	1	3
2MASS J14380829+6408363	16.064	13.906	12.974	12.160	11.659	0.020	0.021	0.022	0.032	0.025	19	1	7
2MASS J14385498−1309103	19.079	16.875	15.528	14.516	13.878	0.022	0.041	0.053	0.049	0.057	26	1	4
2MASS J14493784+2355378	18.761	16.574	15.801	15.069	14.337	0.027	0.082	0.079	0.093	0.099	98	2	4
2MASS J14573965+4517167	15.999	13.954	13.145	12.412	11.923	0.023	0.029	0.027	0.027	0.025	27	1	5
2MASS J15065441+1321060	16.844	14.634	13.414	12.412	11.748	0.017	0.017	0.027	0.031	0.028	13	1	5
2MASS J15261405+2043414	19.044	16.656	15.623	14.501	13.918	0.019	0.046	0.059	0.052	0.059	36	1	4
2MASS J15503820+3041038	15.444	13.765	12.989	12.411	11.924	0.015	0.016	0.030	0.034	0.032	29	1	5
2MASS J15510662+6457047	15.802	13.731	12.870	12.149	11.735	0.016	0.021	0.024	0.029	0.029	22	1	5
2MASS J16000548+1708328	19.236	17.030	16.098	15.129	14.669	0.052	0.158	0.097	0.076	0.122	107	2	4
2MASS J16272794+8105075	16.030	13.995	13.042	12.332	11.874	0.021	0.027	0.024	0.025	0.027	22	1	5
2MASS J16351919+4223053	15.723	13.640	12.886	12.210	11.800	0.021	0.027	0.028	0.032	0.028	24	1	5
2MASS J16561885+2835056	20.589	18.106	16.926	16.269	15.194	0.028	0.093	0.000	0.000	0.146	37	1	4
2MASS J17073334+4301304	17.133	15.005	13.962	13.205	12.657	0.025	0.022	0.025	0.031	0.038	27	1	2
2MASS J17102545+2107155	18.411	16.533	15.867	15.022	14.463	0.023	0.061	0.084	0.090	0.112	109	1	3
2MASS J17114573+2232044	20.730	...	17.100	15.774	14.694	0.030	0.275	0.187	0.113	0.099	44	1	4
2MASS J17281150+3948593	19.684	16.917	15.964	14.781	13.898	0.035	0.086	0.081	0.074	0.052	23	2	4
2MASS J17434148+2127069	19.193	17.044	15.795	14.780	14.290	0.024	0.067	0.086	0.066	0.097	41	1	4
2MASS J17433487+5844110	17.123	14.762	14.016	13.153	12.669	0.037	0.095	0.025	0.030	0.031	30	1	2
2MASS J18410861+3117279	19.746	17.393	16.120	14.970	14.180	0.028	0.056	0.100	0.070	0.084	28	1	4
2MASS J20543585+1519043	19.660	17.485	16.205	15.443	14.811	0.031	0.059	0.107	0.128	0.110	44	1	4
2MASS J20571538+1715154	19.357	17.268	16.107	15.211	14.567	0.031	0.082	0.110	0.090	0.128	63	1	4
2MASS J21011544+1756586	20.677	18.155	16.825	15.792	15.173	0.043	0.188	0.178	0.157	0.194	26	2	4
2MASS J21402931+1625183	15.723	13.764	12.943	12.270	11.779	0.029	0.027	0.031	0.034	0.033	32	2	5
2MASS J21474365+1431315	16.857	14.705	13.842	13.134	12.652	0.051	0.093	0.036	0.032	0.042	40	2	5
2MASS J21580457−1550098	18.559	16.263	14.949	13.916	13.148	0.024	0.060	0.037	0.043	0.040	17	1	8
2MASS J22062280−2047058	15.007	13.197	12.381	11.704	11.325	0.031	0.034	0.026	0.023	0.029	31	2	5
2MASS J22064500−4217210	19.143	16.913	15.569	14.478	13.595	0.028	0.053	0.068	0.056	0.057	25	1	4
2MASS J22081363+2921215	19.588	...	15.818	14.825	14.086	0.028	0.427	0.090	0.083	0.083	17	1	4
2MASS J22244381−0158521	17.759	15.363	14.052	12.803	12.017	0.016	0.034	0.030	0.029	0.029	11.4	1	4
2MASS J22341394+2359559	16.247	14.156	13.176	12.353	11.835	0.031	0.022	0.022	0.030	0.034	22	1	5

TABLE 1—*Continued*

Name	I	Z	J	H	K_s	σ_I	σ_Z	σ_J	σ_H	σ_K	d (pc)	No.	Ref.
2MASS J22425317+2542573	18.124	15.977	14.795	13.754	13.022	0.025	0.031	0.038	0.036	0.038	30	1	1
2MASS J22443167+2043433	20.393	17.678	16.405	14.965	13.932	0.026	0.067	0.128	0.071	0.066	11	1	9
2MASS J23062928−0502285	14.004	...	11.372	10.718	10.288	0.013	...	0.022	0.031	0.027	13	1	5
2MASS J23094618+1549045	17.789	15.847	15.005	14.343	13.907	0.034	0.039	0.059	0.058	0.065	67	1	3
2MASS J23310161−0406193	15.536	13.722	12.937	12.289	11.930	0.027	0.030	0.027	0.027	0.029	28	2	5
2MASS J23494899+1224386	15.320	13.449	12.615	11.952	11.562	0.023	0.022	0.024	0.026	0.030	23	1	5
SDSS J001911.65+003017.8	18.174	15.991	14.924	14.173	13.588	0.020	0.044	0.036	0.034	0.037	37	1	10
2MASS J03440892+0111251*	17.872	15.800	14.725	13.890	13.522	0.017	0.034	0.035	0.036	0.047	40	1	11
SDSSp J104325.10+000148.2	19.255	17.041	16.096	15.111	14.709	0.027	0.059	0.098	0.082	0.120	73	1	12
SDSS J143535.72−004347.0	19.747	17.653	16.461	15.672	15.073	0.022	0.088	0.111	0.115	0.141	70	1	10
SDSS J143517.20−004612.9	19.142	17.202	16.444	15.676	15.268	0.032	0.068	0.104	0.118	0.174	136	1	10
2MASS J15483164−0029414*	18.230	16.532	15.689	15.123	14.850	0.060	0.035	0.067	0.083	0.125	100	1	11
SDSS J165329.69+623136.5	18.371	16.280	15.109	14.389	13.864	0.026	0.033	0.054	0.053	0.067	39	1	10
2MASS J17232861+6406230*	18.961	17.046	16.323	15.644	15.175	0.018	0.051	0.111	0.142	0.191	131	1	11
2MASS J23355849−0013042*	18.735	16.849	15.969	15.206	14.688	0.058	0.091	0.079	0.089	0.104	105	1	11
SDSSp J033035.13−002534.5	18.855	16.520	15.290	14.419	13.829	0.019	0.049	0.045	0.042	0.051	23	1	13
SDSSp J053951.99−005902.0	17.575	15.228	13.986	13.065	12.577	0.019	0.026	0.028	0.028	0.030	12	1	13
2MASS J15154719−0030594*	16.985	15.034	14.181	13.578	13.144	0.016	0.032	0.027	0.028	0.038	45	1	13

REFERENCES.—(1) J. E. Gizis 2002, private communication; (2) K. L. Cruz 2002, private communication; (3) Kirkpatrick et al. 1999; (4) Kirkpatrick et al. 2000; (5) Gizis et al. 2000; (6) J. C. Wilson & K. L. Cruz 2002, private communication; (7) J. D. Kirkpatrick 2002, private communication; (8) C. G. Tinney & J. D. Kirkpatrick 2002, private communication; (9) Dahn et al. 2002; (10) Hawley et al. 2002; (11) G. R. Knapp 2002, private communication; (12) Schneider et al. 2002; (13) Fan et al. 2000.

Table 1 lists composite WFPC2 photometry for those systems. Magnitudes and separations for the individual components in the resolved systems are given in Table 2. Z-band photometry of 2M0335+2342, 2M1711+2232, 2M2208+2921, and 2M2306−0502 was not possible due to cosmic-ray hits. It is possible that low-level cosmic-ray hits might also affect other targets, especially the Z band.

Two of the systems (2M0345+2540 and 2M2224−0158) in our sample have trigonometric parallax measurements (Dahn et al. 2002). For the remainder, we have estimated photometric parallaxes. Unfortunately, the $I-Z$ WFPC2-based colors are not of high enough accuracy to directly estimate photometric distances for each component. Our distances are therefore based on combining the observed I magnitude for the primary, the Reid et al. (2001) I_C-I_{814} relation, and the Dahn et al. (2002) I_C-J, M_J relation.[6] We assume the system $I-J$ color corresponds to the primary's $I-J$ color in order to use the Dahn et al. (2002) relation; we tested differing assumptions such as using the observed system spectral type and got consistent answers. The transformation from separation in arcseconds to AU is uncertain by ~30%; trigonometric parallaxes are needed. These errors have no significance for the interpretation of the data.

Color-color diagrams combining the *HST* and 2MASS photometry are shown in Figures 2 and 3. T dwarfs with

[6] We have adopted this procedure because our new sample adds only one object with an I_C measure and because many of the parallax stars lack WFPC2 measurements.

TABLE 2
DOUBLES

Name	I_A	Z_A	σ_{I_A}	σ_{Z_A}	I_B	Z_B	σ_{I_B}	σ_{Z_B}	P.A.	Sep. (arcsec)	Sep. (AU)
2M1017+1308	18.080	15.905	0.035	0.043	18.260	16.165	0.034	0.045	89	0.100	3
2M1127+7411	16.370	14.478	0.036	0.025	16.803	14.792	0.021	0.023	81	0.250	9
2M1239+5515	19.077	16.675	0.025	0.057	19.104	16.856	0.025	0.055	7	0.213	4
2M1311+8032	16.105	14.223	0.033	0.031	16.328	14.393	0.029	0.024	167	0.300	10
2M1426+1557	16.148	14.108	0.034	0.035	17.291	15.218	0.026	0.023	340	0.155	4
2M1430+2915	18.106	15.947	0.036	0.036	18.628	16.422	0.049	0.048	326	0.084	3
2M1449+2355	19.115	16.984	0.018	0.080	20.151	17.829	0.027	0.113	64	0.133	13
2M1600+1708[a]	19.912	17.644	0.048	0.157	20.072	17.942	0.101	0.218	343	0.056	6
2M1728+3948	20.268	17.802	0.029	0.084	20.636	17.551	0.028	0.110	27	0.130	3
2M2101+1756	21.226	18.579	0.038	0.187	21.681	19.381	0.045	0.343	107	0.232	6
2M2140+1625	16.030	14.130	0.021	0.018	17.245	15.122	0.031	0.043	132	0.158	5
2M2147+1431	17.430	15.305	0.047	0.091	17.825	15.636	0.036	0.048	329	0.323	13
2M2206−2047	15.721	13.940	0.024	0.027	15.799	13.959	0.024	0.024	57	0.160	5
2M2331−0406	15.568	13.784	0.018	0.022	19.363	16.864	0.039	0.066	294	0.576	16

[a] Candidate binary.

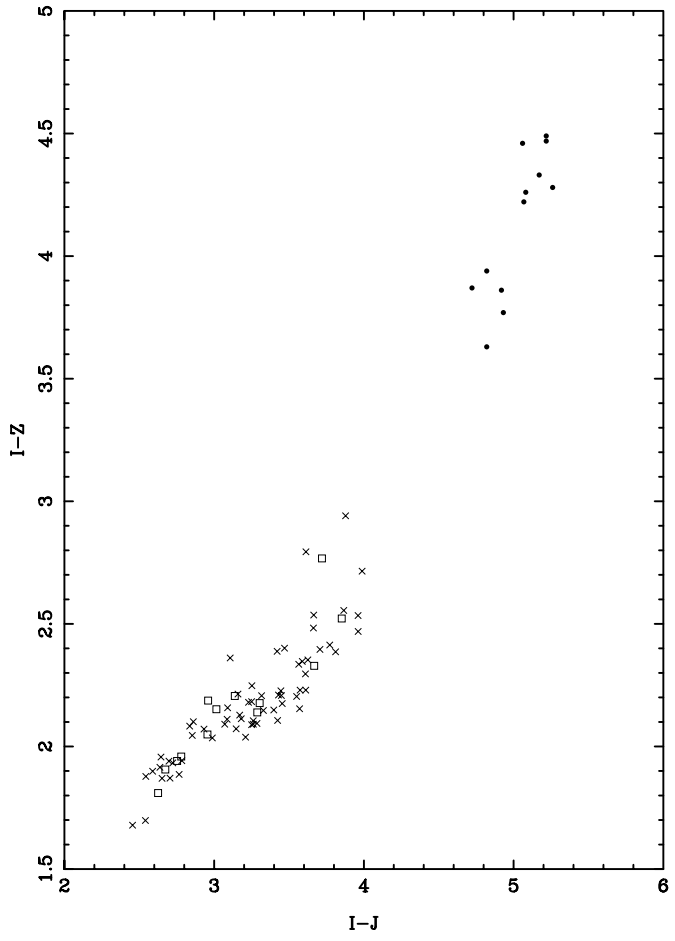

FIG. 2.—Color-color diagram using *HST* (*I*, *Z*) and 2MASS (*J*) photometry. Apparently single dwarfs are shown as crosses and doubles as open squares. T dwarfs from Burgasser et al. (2003) are shown as filled circles.

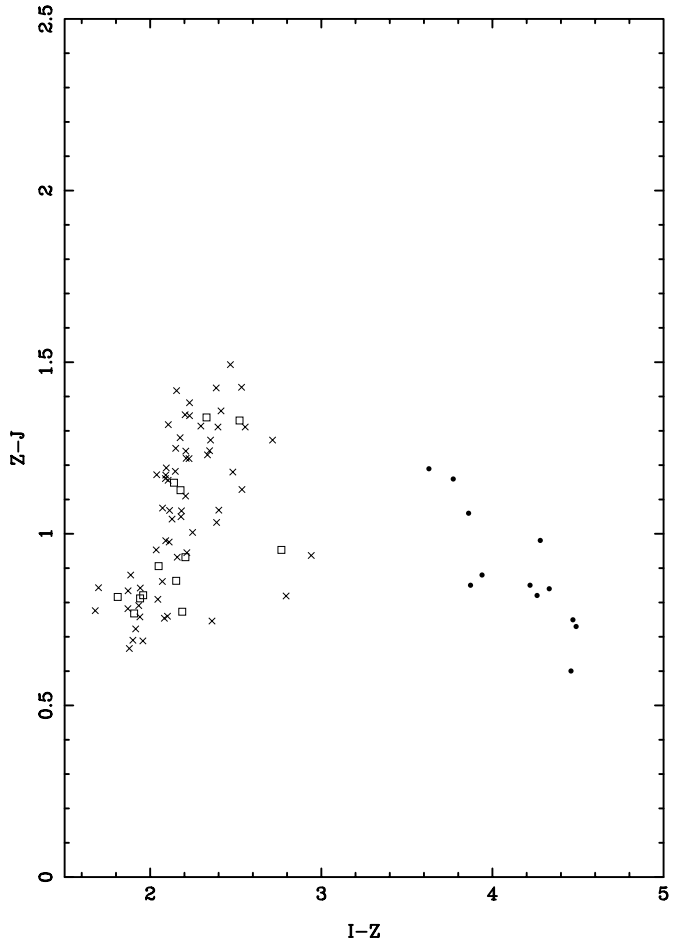

FIG. 3.—Color-color diagram using *HST* (*I*, *Z*) and 2MASS (*J*) photometry. Symbols as in Fig. 2.

WFPC2 photometry by Burgasser et al. (2003) are also shown. The gap between the latest L dwarfs of our program and the T5 and later dwarfs is obvious and is due to the lack of WFPC2 observations of early T dwarfs. Our reddest object in $I-Z$ is the latest L dwarf, the L8 2M0328+2302.

3. INDIVIDUAL SYSTEMS

2M1239+5515: This system shows lithium absorption according to Kirkpatrick et al. (2000), the only resolved binary in this study to do so. As such, both components of the system are below the lithium-burning limit of 0.055–0.060 $M_{\odot}$ (Chabrier & Baraffe 1997; Burrows et al. 2001).

2M1728+3948: This system was classified L7 by Kirkpatrick et al. (2000). Remarkably, component A is brighter by 0.3 mag at *I* but *fainter* by 0.3 mag at *Z* than component B. Component B, with $I-Z$ color of 3.1, is redder than the latest type L dwarfs (Figs. 2 and 3), suggesting that it lies in the L/T transition regime. This behavior invites comparison with observations of late L and early T dwarfs at 1.25 μm, where the latter dwarfs are observed to be brighter by up to 1 mag (Dahn et al. 2002). This has been interpreted as evidence for cloud disruption at the atmospheric temperatures spanned by the L/T transition (Burgasser et al. 2002b). Our observations provide the first evidence that the effect extends down to 1 μm. The primary in this system is cool enough that both components are brown dwarfs, with at least the primary above the lithium-burning limit.

2M1017+1308 and **2M1430+2915**: These two objects were identified as L dwarfs by J. Wilson (2002, private communication) using near-IR spectra. The *HST* colors confirm the cool dwarf classification. Given the spectral types, all of the components could be either stars or brown dwarfs.

2M1449+2355: The limits on lithium for this distant L0 dwarf (Kirkpatrick et al. 2000) system do not rule out its presence. Both components may be stars or brown dwarfs. At 13 AU, this is the most widely separated L dwarf double currently known.

2M1600+1708: LRIS observations of this L1.5 dwarf (Kirkpatrick et al. 2000) system show no evidence for lithium absorption, indicating $M > 0.055$–$0.060\ M_{\odot}$. The *HST* image is better modeled by two PSFs separated by $0\farcs056$ than by a single PSF; we regard this is only a *candidate* double. Additional observations are required to demonstrate that this truly is a binary system.

2M2101+1756: This L7.5 dwarf (Kirkpatrick et al. 2000) system is late enough that both components must be brown dwarfs. The secondary is probably an L8 or slightly later dwarf.

2M1426+1557, **2M2140+1625**, **2M2206−2047**, and **2M2331−0406**: These late M dwarf systems have primaries that are more likely to be stars than brown dwarfs; if any of these systems are young, then the primary may be a brown

dwarf. All four systems were discovered by Close et al. (2002a, 2002b) using Gemini adaptive optics (AO) *J*-, *H*-, and *K*-band imaging, and to whose discussion of individual systems we refer the reader. The *IZ* photometry presented here is consistent with the spectral types expected from the *JHK* photometry. The object 2M2206−2047 has a low tangential velocity (10 km s^{-1}), which is consistent with youth; since many old stars have small velocities, it does not prove youth. Reid et al. (2002) have published a high-resolution spectrum of 2M2206−2047 that shows rapid rotation and no lithium; thus, the possibility that the primary is a high-mass brown dwarf remains viable, but the mass must be above the lithium-burning limit.

2M1127+7411, **2M1311+8032**, and **2M2147+1431**: These late M dwarf systems have primaries that are more likely to be stars than brown dwarfs; if any of these systems are young, then the primary may be a brown dwarf. Using our distance estimate and the Gizis et al. (2000) proper motion, the tangential velocity of 2M1127+7411 is only 6 km s^{-1}; this suggests youth but is not definitive. Our measurements of 2M1127+74AB and 2M1311+80AB are consistent with those reported by Close et al. (2003).

2MASS W0335+2342: This M8.5 dwarf shows lithium absorption and therefore is a young brown dwarf (Reid et al. 2002). Our observations show no evidence for binarity.

4. THE BINARY FRACTION

The most notable characteristic of the data is the lack of wide systems. Even for our faintest, most distant targets, we would have resolved companions with separations greater than 20 AU, yet none are seen. Combining our sample with Reid et al. (2001), we find that zero out of 102 late M and L dwarfs have such companions with $\Delta I < 3$ (and in many cases, $\Delta I < 5$). The 1 σ upper limit on the greater than 20 AU companion frequency is then 1.7%.

Thirteen of the 82 systems in the present sample are resolved as binaries with component separations exceeding our detection thresholds, all in the range 3–16 AU. We have combined these data with the sample of 20 L dwarfs from Reid et al. (2001). Those dwarfs were also identified by color selection from the 2MASS database, and four are clearly resolved as binary systems with $\Delta > 0\farcs06$. This total observed binary fraction of 17^{+4}_{-3}%, where the uncertainties are calculated according to Burgasser et al. (2003), must be corrected to obtain a true binary fraction. First, some of the systems are more distant than others, making the tighter systems unresolvable. The importance of this effect is evident in Figure 4, which shows the magnitudes and colors of the target systems. Four of the 10 systems with $I-K < 4$ and $K < 12$ are resolved as doubles, yet none of the seven systems with $I-K < 4$ and $K > 13.5$ are resolved. The latter are typically 4 times further away, making most double systems unresolvable. Figure 5 plots the histogram of the distance estimates. Overall, excluding the 16 systems in Figure 5 with photometric distances greater than 50 pc, *including the "wide" binary 2M1449+2355 and candidate binary 2M1600+1708*, the observed binary fraction is increased to 19% ± 4%. Nevertheless, we may still fail to resolve many of the systems in the 1.6–10 AU range. This effect biases both the estimate of the binary frequency and the derived binary separation distribution. The observed binary separation distribution is plotted in Figure 6. In order to account for the systems that cannot be resolved, we also weight each system by the number of target systems in which we could have resolved it. For example, the binary 2M1017+1308 could have been resolved, if it had been as close as $0\farcs10$; given our distance estimates, it might have been resolved in only 57 of the total 102 targets searched. The resulting

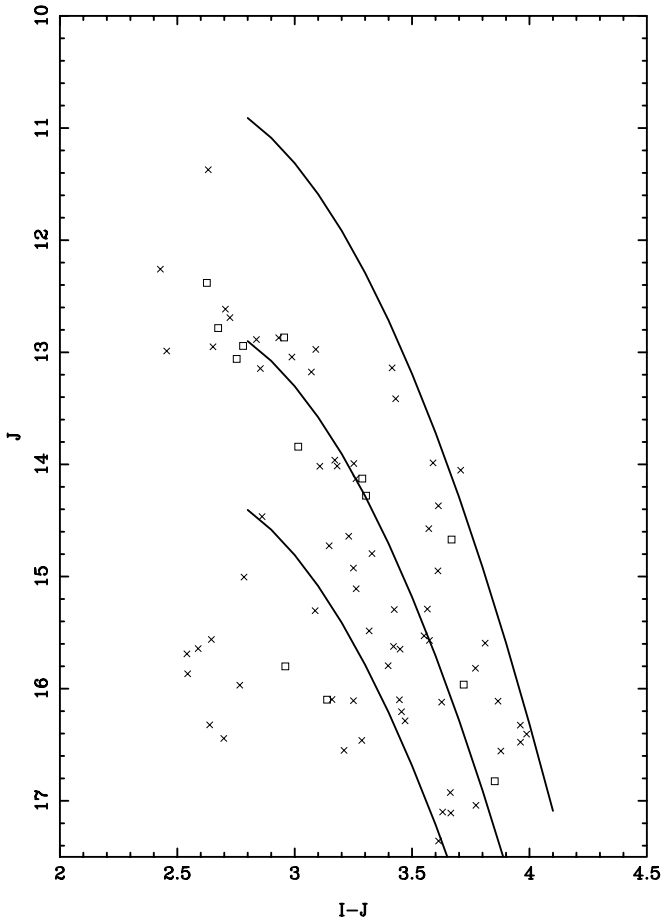

FIG. 4.—Color-magnitude diagram for the sample without corrections for binarity. The apparently single systems appear as crosses and the resolved doubles as open squares. The solid curves plot the Dahn et al. (2002) cool dwarf sequence at distances of 10, 25, and 50 pc.

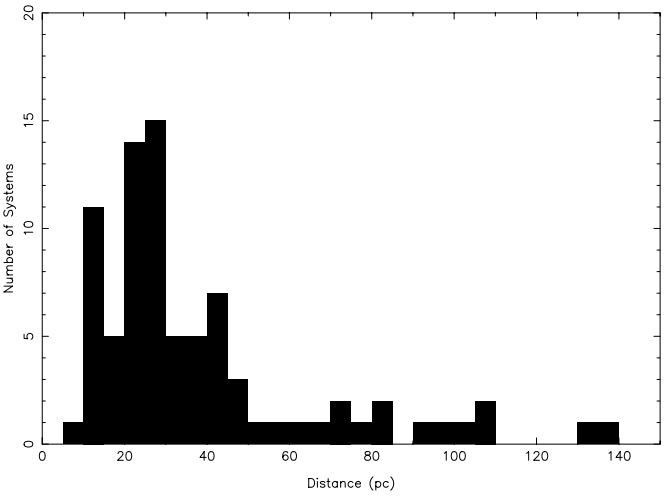

FIG. 5.—Histogram of estimated photometric parallaxes

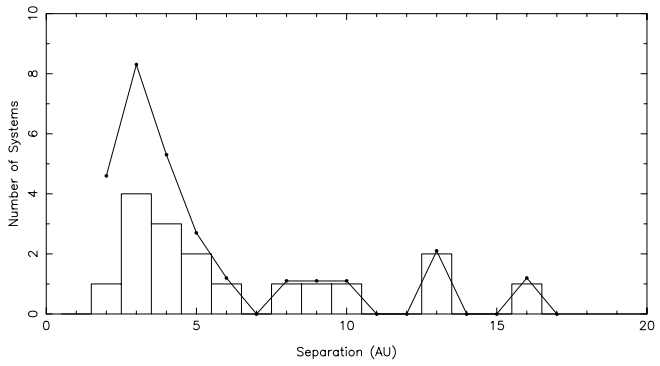

FIG. 6.—Histogram of observed orbital separations. The histogram shows the count of resolved systems, while the filled circles with connecting lines shows the distribution after correction for the fact that the closest systems cannot be resolved in all cases. The distribution is peaked, with companions more common in the range 2–5 AU in the range 6–10 AU.

corrected distribution is also shown in Figure 6. It is evident that binaries in the range ~2–5 AU are more common than the wider systems.

A second important effect is that a luminosity-selected sample such as this one will be afflicted by systematic biases. Two conflicting biases exist (Reid 1991). First, near-equal luminosity binaries can be seen to greater distance and therefore are overrepresented in the sample; if these extra doubles are resolved, they will *increase* the observed binary fraction over the true one. Second, if these extra doubles are not resolved, they will *decrease* the observed binary fraction, since they are counted as single stars. In the case of late M and L dwarfs, where there are no observed systems with separations $\gtrsim$15 AU, the binaries may usefully be considered in two groups: Those with separations in the range 1.6–15 AU and those with separation less than 1.6 AU. Our WFPC2 observations can resolve only the former group (with the innermost limit worse for the more distant objects), but through the second bias effect the latter group can affect our measurements.

The situation can be illustrated by a simple Monte Carlo model. For illustrative purposes only, we consider L dwarfs to be uniformly distributed in space out to a distance of 50 pc to a limiting magnitude of $K_s = 14.0$. In the present schematic model, we assign the same absolute magnitude, $M_K = 11.5$, to each primary. Secondary companions are added to a fraction f_1 of the L dwarfs at separations less than 1 AU (unresolvable) and a fraction f_2 at 1–10 AU (potentially resolvable). The K-band flux ratios are distributed uniformly in the range $0 < \Delta_K < 1$, and the f_2 dwarfs are given true separations between 1.0 and 10.0. If the dwarf(s) have $K < 14$, they are considered as targets, and if they have apparent separation greater than $0''.1$, they are considered to be resolved. We find that in models where the fraction of very close binaries is very large (i.e., $f_1 \gtrsim 0.4$), then the WFPC2-resolved binary fraction is a significant underestimate of the true binary fraction f_2. We therefore must consider what constraints exist on the fraction of very close, near-equal luminosity late M and L dwarf binaries.

Dahn et al. (2002) have published trigonometric parallaxes of 2MASS and DENIS-selected L dwarfs. Of the 17 isolated field L dwarfs in their Table 1, and correcting for the five resolved companions in the range 1–10 AU, only one (2M1328+21) appears to be offset from the L dwarf sequence and may be a close, unresolved double. This system was observed but not resolved by Reid et al. (2001). These data then suggest that $f_1 \lesssim 10\%$. This supported by the scarcity of double-lined binaries detected in high-resolution studies of L dwarfs (Basri et al. 2000; Schweitzer et al. 2001). Similarly, Reid et al. (2002) find two double-lined systems among a sample of 39 M6.5–L0.5 dwarfs. Other results come from studies of the Pleiades. Martín et al. (2000a) estimate that four of 34 of the Pleiades very low mass stars and brown dwarfs are potential near-equal luminosity binaries with separation less than 27 AU based on their positions in the color-magnitude diagram. On the other hand, the double-lined system PPl 15 (Basri & Martín 1999) shows close systems can exist.

The balance of evidence therefore suggests that $f_1 = 5\% \pm 3\%$. It is then likely that the observed binary percentage of $19\% \pm 4\%$ is an overestimate of the true binary fraction (f_2) in the range 1.6–15 AU. We have generated a series of Monte Carlo models similar to the "toy" model described above, but using the observed distance distribution of the sample. By using this observed distance distribution, we include the most important factor in resolving binaries with *HST*. A more advanced treatment of the luminosity differences as a function of separation would be beyond the scope of this paper and would depend on a better understanding of the sample selection effects, the substellar IMF, the L dwarf temperature scale, the star formation history, and other poorly known factors. Our best estimate, based on the simple Monte Carlo models, is that the true value $f_2 = 15\% \pm 5\%$; the decrease due to the bias in including overluminous double is partially offset by the inability to resolve all binaries. On the other hand, the total binary fraction ($f_{\rm tot} = f_1 + f_2$) must be larger than f_2 and is likely to be close to 20% under this model. Potential systematic error is comparable to the random errors due to sample size. In any case, it appears that a binary fraction $f_2 = 15\% \pm 5\%$, with $15\% \leq f_{\rm tot} \lesssim 25\%$. If enough L dwarfs within 10 pc can be discovered, *HST* and/or AO imaging may be able to improve the 1–3 AU constraints.

Since the binary fraction and observed orbital separations of the expanded sample are similar to those in the Reid et al. (2001) sample, the implications of the results remain the same. We refer the reader to Reid et al. (2001) and the more recent Close et al. (2003) for a discussion of the similarities and differences of the M and L dwarf binaries relative to main-sequence stars. In particular, the lack of systems at greater than 20 AU is now highly significant and a major difference from mid M (Fischer & Marcy 1992) and G dwarfs (Duquennoy & Mayor 1991), as seen in Figure 7. A well-defined sample of M5–M6.5 dwarfs would allow the question of continuity of the binary frequency and orbital separation distribution to be addressed.

Since we cover late M, nonlithium L, and lithium L dwarfs, we may search for differences as a function of mass of the primary. In other words, we address the question "does the binary fraction vary with mass near the hydrogen-burning limit?" Ten L dwarf systems in this study and Reid et al. (2001) have spectroscopic detections of lithium, placing them below the lithium-burning limit (~0.055 $M_\odot$).[7] Three are doubles. Given the small sample size, the resulting

[7] Three other L dwarf systems, all apparently single, have marginal lithium detections.

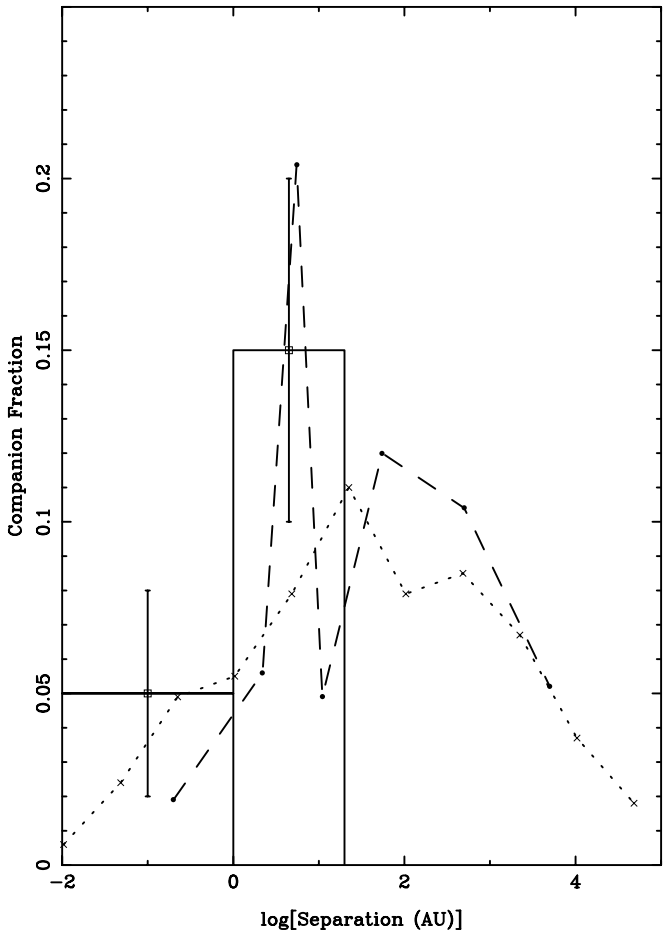

FIG. 7.—Derived binary fractions for late M and L dwarfs compared with early M dwarfs (*long-dashed lines*, Fischer & Marcy 1992) and G dwarfs (*short-dashed lines*, Duquennoy & Mayor 1991); all stellar companions regardless of mass ratio are included. Note the lack of wide companions and the relative "excess" of 1–16 AU companions for the coolest primaries relative to the G dwarfs.

binary fraction (30%) is consistent with that of the non-lithium L dwarfs and the late M dwarfs. There is no evidence of a strong variation in binary frequency over the mass range $\sim$0.08 to $\sim$0.04 $M_{\odot}$. It is interesting to note that all the doubles with companions in the range 10–16 AU have M8–L0 (probably stellar) dwarf primaries, while all of the later L and lithium L (brown) dwarfs are tighter systems. Additional data are needed to assess the currently marginal significance of this effect. Our results are consistent with Burgasser et al. (2003)'s sample of 10 T (brown) dwarfs in both the frequency and orbital separation. In particular, the fact that both of the resolved T dwarfs have separations less than 5 AU is consistent with the peak seen for the late M and L dwarfs separations in Figure 6.

5. SUMMARY AND CONCLUSIONS

We have identified 13 definite and one candidate late M and L dwarf binaries in a sample of 82 2MASS- and SDSS-selected field dwarfs. Including the 20 Reid et al. (2001) target systems, the observed binary fraction is 17^{+4}_{-3}%. We argue that accounting for biases and incompleteness leads to an estimated binary fraction $15\% \pm 5\%$. No systems wider than 20 AU are found. Within the limits of the small sample sizes, we find no evidence for variations as a function of mass in the binary fraction. Our results are consistent with the (largely overlapping) late M sample of Close et al. (2003) and the T dwarf sample of Burgasser et al. (2003).

Additional near-infrared observations of the brown dwarf double 2M1728+3948 are needed. We interpret the secondary as an early T dwarf. Orbital motions for these systems should be detectable using *HST*. This offers the opportunity to determine masses.

The greatest need for the future is a better defined sample of L dwarf targets, such as a 2MASS-selected sample of bright L dwarfs (Cruz et al. 2003). The current sample of L dwarfs, although large, was not selected with consistent magnitude and color cuts that have well-understood effects. Once such a sample is available with *HST* or AO data, the bias and selection effects can be better understood.

Based on observations made with the NASA/ESA *Hubble Space Telescope*, obtained at the Space Telescope Science Institute, which is operated by AURA, Inc., under NASA contract NAS 5-26555. These observations are associated with proposal 8581. Support for this work was provided by NASA through grant number HST-GO-08581.01-A from the Space Telescope Science Institute. This publication makes use of data products from 2MASS, which is a joint project of the University of Massachusetts and Infrared Processing and Analysis Center, funded by NASA and NSF.

REFERENCES

Basri, G., & Martín, E. L. 1999, AJ, 118, 2460
Basri, G., Mohanty, S., Allard, F., Hauschildt, P. H., Delfosse, X., Martín, E. L., Forveille, T., & Goldman, B. 2000, ApJ, 538, 363
Burgasser, A. J., et al. 2002a, ApJ, 564, 421
Burgasser, A. J., Kirkpatrick, J. D., Reid, I. N., Brown, M. E., Miskey, C. L., & Gizis, J. E. 2003, ApJ, 586, 512
———. 2002b, ApJ, 571, L151
Burrows, A., Hubbard, W. B., Lunine, J. I., & Liebert, J. 2001, Rev. Mod. Phys., 73, 719
Chabrier, G., & Baraffe, I. 1997, A&A, 327, 1039
Close, L. M., Potter, D., Brandner, W., Lloyd-Hart, M., Liebert, J., Burrows, A., & Siegler, N. 2002a, ApJ, 566, 1095
Close, L. M., Siegler, N., Freed, M., & Biller, B. 2003, ApJ, 587, 407
Close, L. M., Siegler, N., Potter, D., Brandner, W., & Liebert, J. 2002b, ApJ, 567, L53
Cruz, K. L., et al. 2003, in preparation
Cutri, R. M., et al. 2000, Explanatory Supplement to the 2MASS Second Incremental Data Release (Pasadena: IPAC)
Dahn, C. C., et al. 2002, AJ, 124, 1170
Delfosse, X., et al. 1997, A&A, 327, L25
Dolphin, A. E. 2000, PASP, 112, 1397
Duquennoy, A., & Mayor, M. 1991, A&A, 248, 485
Epchtein, N. 1997, in The Impact of Large Scale Near-IR Sky Surveys, ed. F. Garzon et al. (Dordrecht: Kluwer), 15
Fan, X., et al. 2000, AJ, 119, 928
Fischer, D. A., & Marcy, G. W. 1992, ApJ, 396, 178
Geballe, T. R., et al. 2002, ApJ, 564, 466
Gizis, J. E., Monet, D. G., Reid, I. N., Kirkpatrick, J. D., Liebert, J., & Williams, R. J. 2000, AJ, 120, 1085
Gizis, J. E., & Reid, I. N. 1995, AJ, 110, 1248
Halbwachs, J. L., Arenou, F., Mayor, M., Udry, S., & Queloz, D. 2000, A&A, 355, 581
Hawley, S. L., et al. 2002, AJ, 123, 3409
Holtzman, J. A., Burrows, C. J., Casertano, S., Hester, J. J., Trauger, J. T., Watson, A. M., & Worthey, G. 1995, PASP, 107, 1065
Joyce, R. 1999, The CRSP User's Manual (Tucson: KPNO)
Kirkpatrick, J. D., Reid, I. N., Gizis, J. E., Burgasser, A. J., Liebert, J., Monet, D. G., Dahn, C. C., & Nelson, B. 2000, AJ, 120, 447

Kirkpatrick, J. D., et al. 1999, ApJ, 519, 802
Koerner, D. W., Kirkpatrick, J. D., McElwain, M. W., & Bonaventura, N. R. 1999, ApJ, 526, L25
Marcy, G. W., & Butler, R. P. 2000, PASP, 112, 137
Martín, E. L., Brandner, W., & Basri, G. 1999a, Science, 283, 1718
Martín, E. L., Brandner, W., Bouvier, J., Luhman, K. L., Stauffer, J., Basri, G., Zapatero Osorio, M. R., & Barrado y Navascués, D. 2000a, ApJ, 543, 299
Martín, E. L., Delfosse, X., Basri, G., Goldman, B., Forveille, T., & Zapatero Osorio, M. R. 1999b, AJ, 118, 2466
Martín, E. L., Koresko, C. D., Kulkarni, S. R., Lane, B. F., & Wizinowich, P. L. 2000b, ApJ, 529, L37
Potter, D., Martín, E. L., Cushing, M. C., Baudoz, P., Brandner, W., Guyon, O., & Neuhauser, R. 2002, ApJ, 567, L133
Reid, I. N., Gizis, J. E., Kirkpatrick, J. D., & Koerner, D. W. 2001, AJ, 121, 489
Reid, I. N., et al. 1999, ApJ, 521, 613
Reid, I. N., Kirkpatrick, J. D., Liebert, J., Gizis, J. E., Dahn, C. C., & Monet, D. G. 2002, AJ, 124, 519
Reid, N. 1991, AJ, 102, 1428
Schneider, D. P., et al. 2002, AJ, 123, 458
Schweitzer, A., Gizis, J. E., Hauschildt, P. H., Allard, F., Howard, E. M., Kirkpatrick, J. D. 2002, ApJ, 566, 435
Schweitzer, A., Gizis, J. E., Hauschildt, P. H., Allard, F., & Reid, I. N. 2001, ApJ, 555, 368
Skrutskie, M. F., et al. 1997, in The Impact of Large Scale Near-IR Sky Surveys, ed. F. Garzon et al. (Dordrecht: Kluwer), 25
York, D. G., et al. 2000, AJ, 120, 1579